Seamon, K. B. (1980) *Biochemistry 19*, 207–215.
Tanaka, T., & Hidaka, H. (1980) *J. Biol. Chem. 255*, 11078–11080.
Van Eldik, L. J., Zendegu, J. G., Marshak, D. R., & Watterson, D. M. (1982) *Int. Rev. Cytol. 77*, 1–61.
Walsh, M. P., Stevens, F. C., Oikawa, K., & Kay, C. M. (1978) *Biochemistry 17*, 3928–3930.
Wasserman, R. H., Fullmer, C. S., & Taylor, A. N. (1978) in *Vitamin D* (Lawson, D. E. M., Ed.) pp 133–166, Academic Press, New York.

Refined Crystal Structure of Calcium-Liganded Carp Parvalbumin 4.25 at 1.5-Å Resolution†

Vinod D. Kumar,‡ Lana Lee,§ and Brian F. P. Edwards*,‡

Department of Biochemistry, Wayne State University School of Medicine, Detroit, Michigan 48201, and Department of Chemistry and Biochemistry, University of Windsor, Windsor, Canada N9B 3P4

Received June 6, 1989; Revised Manuscript Received October 9, 1989

ABSTRACT: The crystal structure of carp parvalbumin (pI = 4.25) has been refined by restrained least-squares analysis employing X-ray diffractometer data to 1.5-Å resolution. The final residual for 12 653 reflections between 10 and 1.5 Å with $I(hkl) > 2\sigma(I)$ is 0.215. A total of 74 solvent molecules were included in the least-squares analysis. The root mean square deviation from ideality of bond lengths is 0.024 Å. The model has a root mean square difference of 0.59 Å from the positions of the main-chain atoms in a previously reported structure [Moews, P. C., & Kretsinger, R. H. (1975) *J. Mol. Biol. 91*, 201–228], which was refined by difference Fourier syntheses using data collected by film to 1.9 Å. Although the overall features of the two models are very similar, there are significant differences in the amino-terminal region, which was extensively refit, and in the number of oxygen atoms liganding calcium in the CD and EF sites, which increased from six to seven in the CD site and decreased from eight to seven in the EF site.

Parvalbumins are small, calcium-binding proteins that are found primarily in the muscle tissue of vertebrates. Their properties include acidic isoelectric points, amino acid compositions rich in phenylalanine and alanine, and binding sites for 2 mol of calcium/mol of protein with dissociation constants of 10^{-7}–10^{-9} M [reviewed in Kretsinger (1980)]. Calcium-binding parvalbumin was first identified in frog muscle by Deuticke (1934) and further characterized by Hamoir (1951). Parvalbumins have now been isolated from the muscles of a wide variety of fish such as carp (Konusu et al., 1965), hake (Pechère et al., 1971), pike (Rao & Geraday, 1973), and other vertebrates such as frog (Pechère et al., 1973) and chicken (Heizmann & Strehler, 1979). A parvalbumin has also recently been identified in the γ-aminobutyric acid containing cells of the rat cerebral cortex (Celio, 1986). Besides carp 4.25 parvalbumin, crystal structures have been reported for *Opsanus tau* parvalbumin (Kahn et al., 1985) and pike 4.1 parvalbumin (Declercq et al., 1988).

The physiological role of parvalbumins has remained obscure for a long time, since these proteins are not involved in glycolysis or osmotic regulation, nor do they serve any known nutritional role. However, several inferences have been made on the basis of their location and strong metal-binding capacities. For example, parvalbumins are associated with only certain types of muscles such as fast nerve impulse activated skeletal muscles, which suggests they are not part of the contractile machinery but are instead connected with the calcium-dependent regulation of this type of muscle. For example, mouse mutants deficient in parvalbumin exhibit tetanic contractures after the cessation of motorneuron stimulation (Stuhfauth et al., 1984). In the rat, the parvalbumin gene has promoter sequences that are homologous to conserved sequences in the promoter region of myosin light chain, suggesting a common mechanism for regulation (Berchtold et al., 1987).

There is also evidence that the function of parvalbumins is not limited to muscle cells alone. Parvalbumin has been localized specifically in γ-aminobutyric acid containing cells in the brain (Celio, 1986), and chicken thymic hormone, which is very similar in its physical and chemical properties to mammalian thymosins and thymopoietins, has been identified as a parvalbumin (Brewer et al., 1989). This latter paper is the first instance of an unequivocal, specific function for a parvalbumin and suggests that parvalbumins have a role in development of the immune system.

Five parvalbumins have been isolated from carp muscle with isoelectric points of <3.9, 3.95, 4.25, 4.37, and 4.47 (Pechère et al., 1971). They have been labeled as parvalbumins 1, 2, 3, 5a, and 5b, respectively (Pechère et al., 1971). Another notation (Coffee et al., 1974), which originated in the order of elution from an anion-exchange column, is parvalbumin A_1 (pI = 4.47), A_2 (pI = 4.37), B (pI = 4.25), C (pI = 3.95), and D (pI < 3.9). We have followed the practice of Declercq et al. (1988) and identified the parvalbumins by their isoelectric points. Carp 4.25 parvalbumin was sequenced by Coffee and Bradshaw (1973). The protein contains 108 amino acid residues, an acetylated amino terminus, and high amino acid compositions of alanine (20%), phenylalanine (10%), and lysine (10%). The three-dimensional crystal structure was determined by Kretsinger and Nockolds (1973) to 1.9-Å resolution by the multiple isomorphous replacement method. The structure was subsequently refined by Moews and Kretsinger (1975), at the same resolution by a real space refinement procedure of Diamond (1971). Their crystal structure analysis

† This work was supported in part by NIH Grants GM 33192 and RR 02945, a grant from NSERC, and a grant-in-aid from the WSU Center for Molecular Biology.
‡ Wayne State University School of Medicine.
§ University of Windsor.

0006-2960/90/0429-1404$02.50/0

revealed six helical regions, which they labeled A–F. The two calcium sites had the same structural motif, called either a "EF hand" (Kretsinger & Nockholds, 1973) or a "calmodulin fold" (Kretsinger, 1987), which was formed by an α-helix linked to a second α-helix by a 12-residue loop around the metal ion. The loops between helices C and D and between helices E and F each bound a calcium ion using carbonyl, carboxyl, and hydroxyl oxygens.

In this paper, we present the refinement of the crystal structure of carp 4.25 parvalbumin at 1.5-Å resolution by a restrained least-squares procedure (Hendrickson & Konnert, 1980). We undertook this study to establish a reference structure for later comparison with that of ytterbium-substituted parvalbumin determined by nuclear magnetic methods (Lee & Sykes, 1983).

Experimental Procedures

Crystal Growth and Treatment. Carp 4.25 parvalbumin was prepared by the method of Pechère et al. (1971). Crystals of parvalbumin were grown at room temperature by the micro vapor diffusion or hanging drop method in Lindbro tissue culture plates or in nested crystallization dishes (McPherson, 1982). A parvalbumin solution (22 mg/mL) was prepared by dissolving lyophilized protein in 12.5 mM PIPES[1] buffer that had been adjusted to pH 6.56 with HCl. It was passed through a 0.45-μm filter before crystallization. The protein concentration was checked by using a value of 0.173 for $E_{1\%}$ at 259 nm (Pechère et al. 1971). Aliquots (10–40 μL) of the protein solution were mixed with equal volumes of 65–70% saturated ammonium sulfate buffered at pH 6.56 with 10 mM PIPES and equilibrated at ambient temperature by vapor diffusion with a reservoir of the ammonium sulfate solution.

The protein crystals appeared in 2 weeks and continued to grow for a month. The crystals were stabilized by an aliquot of 60% saturated ammonium sulfate, pH 6.56, that was 10 times the volume of the drop. The crystals, which are isomorphous with those of Kretsinger and Nockolds (1973), belonged to the monoclinic space group C2, with unit cell parameters $a = 28.55 \pm 0.01$ Å, $b = 60.91 \pm 0.02$ Å, $c = 54.42 \pm 0.01$ Å, and $\beta = 94.86 \pm 0.01°$ as calculated by least-squares from 14 reflections that were refined on the diffractometer. There is one molecule per asymmetric unit.

Data Collection and Processing. Intensity measurements on carp parvalbumin crystals were recorded on a Syntex $P2_1$ four-circle diffractometer using nickel-filtered Cu Kα radiation at 40 kV and 26 mA. The intensities were measured by using an ω scan (Wyckoff et al., 1967). Each reflection was scanned for 45 s in 11 steps of 0.03° each and the 7 largest, contiguous counts were summed to give the net count. The crystals were mounted with the b^* axis along the spindle axis. The alignment of the crystal during data collection was monitored by remeasuring five reflections, which were distributed evenly across the 2θ range of the data set, every 200 reflections. Three of the monitored reflections (used in alignment) were located along the three axes so that motion or slippage in any direction was easily detected. The crystal was realigned automatically whenever the intensity of a monitor reflection fell below 90% of its original value. The radiation damage as a function of time was calculated by averaging the slopes of the least-squares straight lines that best fitted the multiply measured intensities of the same five reflections.

[1] Abbreviations: rms, root mean square; PIPES, piperazine-*N*,*N*'-bis(2-ethanesulfonic acid); merging residual, $\sum_{i=1,N}\sum_{k=1,n}(I_k - \langle I\rangle_i)/\langle I\rangle_i$, where $\langle I\rangle_i$ is the average of n duplicate measurements of the ith reflection and there are N unique reflections.

Table I: Summary of the Refinement of Carp Parvalbumin Structure

cycles	data (Å)	R factor[a]	water molecules
start	5.0–3.0	0.399	
1–12[b]	5.0–3.0	0.231	
13–16	5.0–2.5	0.274	
17–20	5.0–2.0	0.293	
21–23	5.0–1.8	0.298	
24–25	5.0–1.65	0.290	
26–39	5.0–1.5	0.269	
40–43	10.0–1.5	0.274	
44–47[c]	10.0–1.5	0.267	
48–52[d]	10.0–1.5	0.262	
53–57	10.0–1.5	0.233	52
58–62[e]	10.0–1.5	0.219	98
63–67	10.0–1.5	0.215	88
68–70	10.0–1.5	0.213	98
71–76[f]	10.0–1.5	0.217	84
77–79	10.0–1.5	0.216	79
80–82[g]	10.0–1.5	0.215	79
83	10.0–1.5	0.215	74
84–87[h]	10.0–1.5	0.247	74

[a] $R = \sum||F_o| - |F_c||/\sum|F_o|$. [b] All 812 atoms of the protein were included for cycles 1–43. The two calcium atom were included in cycles 1–87. [c] All atoms for residues 1–5, and the atoms beyond C_β for residues 41, 79, 83, and 87 were omitted. [d] Atoms beyond C_β for residues 41, 79, 83, and 87 were omitted. [e] Residues 1–5 were included. [f] All 812 atoms of the protein were included for cycles 71–83. [g] Refinement of the occupancies and temperature factors of the solvent. [h] Atoms beyond C_β for residues 51, 53, 55, 57, 59, and 62 of the CD metal-binding site and for residues 90, 92, 94, 96, and 101 of the EF metal-binding site were omitted.

Structure Analysis. Electron density maps were interpreted on a MMSX graphics system using the M3 program (Sielecki et al., 1982). The final model was analyzed with the QUANTA program (Polygen Corp.) on a Iris 4D70 graphics workstation.

Results

The data to 1.5-Å resolution were collected from two crystals. The first crystal was used to collect a total of 6871 intensities that were greater than twice their estimated standard errors from infinity to 1.9 Å. The second crystal was similarly used to record 7352 reflections in the 2.0–1.5-Å range. The radiation damage at the end of the data collection was 9% on crystal 1 and 14% on crystal 2. The measured intensities from each crystal were corrected for decay, background scattering, Lorentz polarization, and absorption (North et al., 1968). The symmetry residual was 0.036 for 347 symmetry-related observations on crystal 1 and 0.094 for 197 observations on crystal 2. The absorption-corrected intensity data from the two crystals were merged with the ROCKS programs (Reeke, 1984) and placed on a common scale using 901 reflections in the overlapping range 2.0–1.9 Å. The merging residual (defined in footnote 1) from ROCKS was 0.081; the final data set contained 12 653 reflections with intensities greater than 2σ of a possible 14 318 reflections.

Progress of Refinement. The F6A set of atomic coordinates of Moews and Kretsinger (1975) was chosen as the starting point for the refinement because it had the lowest residual while still retaining idealized geometry. The first stage of restrained least-squares refinement was initiated with a 5.0–3.0-Å data set with an overall temperature factor of 14 Å^2. The course of the refinement is summarized in Table I. Twelve cycles of refinement were undertaken to bring the R factor from 0.399 to 0.231. At this point individual temperature factors were included in the refinement scheme. Twenty-seven cycles of refinement were undertaken by using the 3.0–1.5-Å data set. Data from 3.0 to 1.5 Å were divided into five shells (3.0–2.5, 2.5–2.0, 2.0–1.8, 1.8–1.65, 1.65–1.5)

and added sequentially to give an R factor of 0.269.

At this point intensity data in the 10.0–5.0-Å range were included in the refinement. Four additional cycles of refinement were undertaken to give an R value of 0.274 for the complete 10.0–1.5-Å resolution data. Fourier maps using $2F_o - F_c$ as coefficients were calculated and examined on a graphics system. The electron density was weak for residues 1–5 and the side-chain atoms of Asp-41, Asp-79, Lys-83, and Lys-87. These residues and side chains were excluded in the next series of refinement calculations. Four cycles of refinement reduced the R value from 0.274 to 0.267. An $F_o - F_c$ electron density map showed unambiguous density for the main chain of residues 1–5. Five cycles of refinement with the refit amino-terminal region reduced the R factor to 0.262. The new electron density still had some areas of fragmented density at the amino terminus.

At this stage a real space solvent search program was used to locate peaks in an $F_o - F_c$ map that had heights greater than 3 times the standard deviation of the map and were within 2.5–3.5 Å of a hydrogen-bonding atom of the protein or a previously included water molecule. A total of 52 acceptable peaks were found. They were included in the next round of structure factor and least-squares calculations, with the side-chain atoms of residues Asp-41, Asp-79, Lys-83, and Lys-87 still omitted. Five cycles of refinement reduced the R value from 0.262 to 0.233. Electron density maps were recalculated and analyzed on the graphics system. The N-acetyl group, which had been left out of the refinement calculations, could be located from these maps and was fit into density. A few water molecules were manually adjusted to bring them into density, while others were deleted because they had no density associated with them. The peak search program was used to locate additional water peaks. At this stage a total of 98 water molecules were included in the least-squares refinement, and five cycles of least-squares reduced the R value to 0.219. A total of eight cycles in two stages with addition and substitution of water molecules reduced the R value to 0.213. The model at this stage consisted of 798 protein atoms and 98 water peaks. A total of 14 water peaks were removed because they belonged to other asymmetric units. Nine cycles of refinement, including the side-chain atoms of residues 41, 79, 83, and 87, were undertaken to give an R factor of 0.216. A check for intermolecular contacts revealed five more symmetry-related water molecules, which were deleted. As a last step, the occupancies of the 79 water molecules were refined in four cycles to give an R factor of 0.215. Five water molecules not in density were removed; the remaining water molecules had occupancies greater than 0.6. The final, overall R factor for the model, including all residues, two calcium atoms, and 74 water molecules, is 0.215 for 12653 reflections with $I > 2\sigma(I)$ in the 10.0–1.5-Å resolution range. The phasing statistics are presented by shells in Table II. The rms shift in atomic positions in the last cycle was 0.025 Å. In the final model, the rms deviation of bond lengths from ideality is 0.024 Å, the rms deviation from planarity for 146 planar groups is 0.01 Å, and the rms deviation for the 108 peptide bond torsional angles is 1.9°. Only 69 of 2188 bond distances deviate by more than 0.03 Å from ideal values. In our refined model, eight residues on the surface of parvalbumin, namely, Lys-32, Lys-45, Lys-83, Lys-87, Asp-61, Asp-79, Ser-39, and Gln-52, have one or more atoms not in density. The only main-chain residue with weak density is Ala-3.

Because the coordination of the calcium ions had changed in both the CD and EF sites, we undertook four extra cycles of refinement in which the side-chain atoms beyond the C_β position were excluded for all residues that directly liganded calcium, namely, Asp-51, Asp-53, Ser-55, Phe-57, Glu-59, Glu-62, Asp-90, Asp-92, Asp-94, Lys-96, and Glu-101. Analysis of the resulting $F_o - F_c$ electron density map showed that these atoms were fit correctly to the observed density. We also examined the effect of restricting the data to the best phased shells in Table II. When the final 1.5-Å model was subjected to a further 14 cycles of refinement using only the 5–1.9-Å data, the R factor was 0.182 with an 0.024 deviation in bond lengths. Although the electron density for the amino terminus and for the calcium ligands was less resolved due to the lower resolution, it agreed in all essentials with the 1.5-Å maps whether or not residues 1–4 or the ligands beyond the C_β carbon were included.

Table II: Summary of the Refinement Statistics

resolution (Å)	no. of reflections obsd[a]	% [b]	R factor
10.00–5.00	359	93.4	0.286
5.00–3.00	1460	95.3	0.186
3.00–2.50	1319	94.8	0.205
2.50–2.00	2843	90.9	0.201
2.00–1.80	2146	91.3	0.235
1.80–1.65	2130	81.5	0.258
1.65–1.50	2396	64.9	0.260

[a] Reflections with $F > 2\sigma$. [b] Percent of the total possible reflections in the shell that were observed with $F > 2\sigma$.

Discussion

As expected, our refined model has the same overall features that were observed by Moews and Kretsinger (1975) in their model at 1.9 Å. The parvalbumin molecule has approximate dimensions 31 × 40 × 25 Å and six helices (A–F) with a loop between each pair. The two calcium-binding sites at the CD and EF loops are formed from a continuous polypeptide sequence containing two turns of helix, a 12-residue loop around the metal, and a second two-turn helix. Figure 1, which was calculated by using the program OVERLAP (Rossmann & Argos, 1975), shows a least-squares superposition of the C_α atoms of our 1.5-Å model and the 1.9-Å model of Moews and Kretsinger (1975). The F6A coordinates (R factor = 0.40) in the Brookhaven Protein Data Bank (file 1CPV; Bernstein et al., 1977), which were used by Moews and Kretsinger (1975) in their analysis of the calcium-binding sites, have also been used in this discussion unless stated otherwise. The first five residues, which were rebuilt in the 1.5-Å structure, had a rms difference of 4.04 Å. Other regions of four or more residues that had a local rms deviation above 0.80 Å occurred at residues 34–39 between the B and C helices and at residues 63–66 of the D helix.

The locations of N-acetylated Ala-1 and the side chain of Phe-2 were particularly problematic in the 1.9-Å model. Originally the Ala-1 N-acetyl group was tucked into a pocket and the Phe-2 side chain was on the surface (Nockolds et al., 1972; Kretsinger & Nockolds, 1973). Later the positions were reversed on the basis of a spectrophotometric pH titration of Tyr-2 in carp 3.95 parvalbumin which suggested that the phenol group was buried because its pK_a increased 1.25 units upon denaturation with urea (Coffee et al., 1974; Moews & Kretsinger, 1975). However, our electron density (Figure 2, top) supports the original structure (Nockolds et al., 1972) with Phe-2 on the surface and Ala-1 in the buried position where the nitrogen of N-acetylated Ala-1 can hydrogen bond to the carbonyl of Asn-69. Possibly, in parvalbumin 3.95 it is Tyr-2 that hydrogen bonds to Asn-69.

Residues 34–39, which have an average rms difference of 0.83 in Figure 1, are part of a surface loop. The concerted

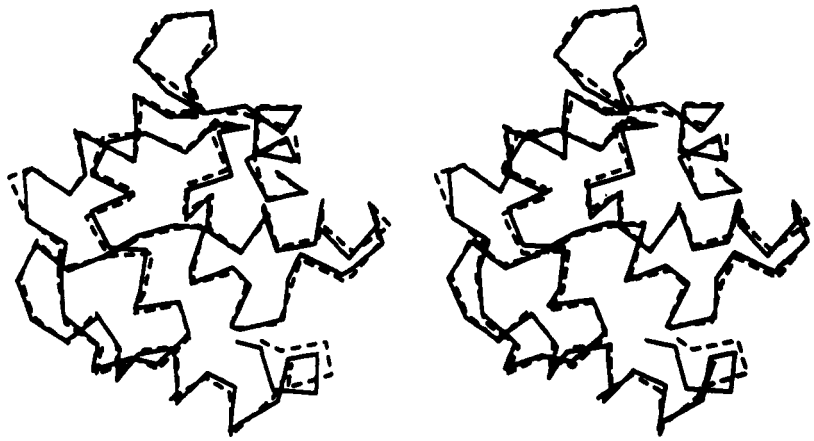

FIGURE 1: Comparison of the C_α backbone. The 108 C_α carbons of the 1.5- (solid lines) and 1.9-Å (dashed lines) models are shown in stereo. The backbones were overlapped by a least-squares calculation using all 108 C_α carbons. The rms deviation in the coordinates was 0.59 Å; it was 0.57 Å with residues 1–5 (bottom right in the figure) omitted from the calculation.

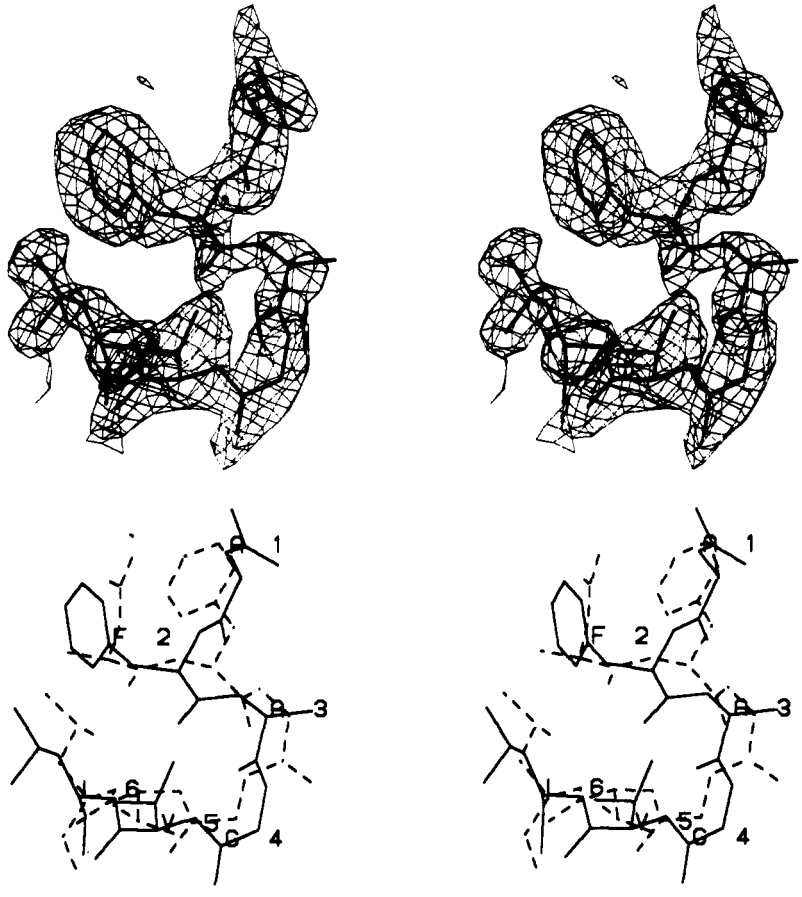

FIGURE 2: Amino terminus. (Top) Residues Ala-1–Leu-6 from the refined model of carp parvalbumin at 1.5-Å resolution are superimposed on the $2F_o - F_c$ electron density map. (Bottom) Residues Ala-1–Leu-6 from the 1.5- (solid lines) and 1.9-Å (dashed lines) models are shown in stereo. The major differences are in the ψ_2 and ϕ_5 torsion angles, which differ by 152° and 144°, respectively. The overlap of the two structures was calculated by least-squares from the positions of all 108 C_α carbons.

movement at these positions cannot be ascribed to any dramatic change in the structure. In the 1.9-Å model, the carboxyl oxygens of residues 36 and 38 form hydrogen bonds to the side chain of Lys-107, whereas in the 1.5-Å structure only residue 38 does. The side chain of Ser-39 is hydrogen bonded to the side chain of Asp-42 in the 1.5-Å model but not in the 1.9-Å structure.

Residues 63–66 have an average rms difference of 0.85 Å in Figure 1. This movement reflects the fact that helix D has a less pronounced bend at residue 65 in the 1.5-Å model.

Hydrogen Bonding. Figure 3 compares the main-chain, intramolecular hydrogen bonds, as assigned by the QUANTA program using the criteria of Baker and Hubbard (1984), for our model and for the F6A model of Moews and Kretsinger (1975). We did not rely exclusively on the assignment of hydrogen bonds made by Moews and Kretsinger for the 1.9-Å structure because the data in their Table 6 were not consistent. For example, a bond listed by Moews and Kretsinger between Ser-37 and Thr-36 has N→O = 3.0 Å, H→O = 2.3 Å, and N–O–H = 38°. These numbers give a N→H distance of 1.85 Å. The accepted value is 1.0 Å (Creighton, 1984). By the criteria of Baker and Hubbard (1984), 64 of the 108 peptide NH groups in the 1.5-Å model have at least one hydrogen bond with a main-chain carbonyl group and another 15 are hydrogen bonded solely to side-chain atoms. In the F6A model of Moews and Kretsinger, the corresponding numbers are 52

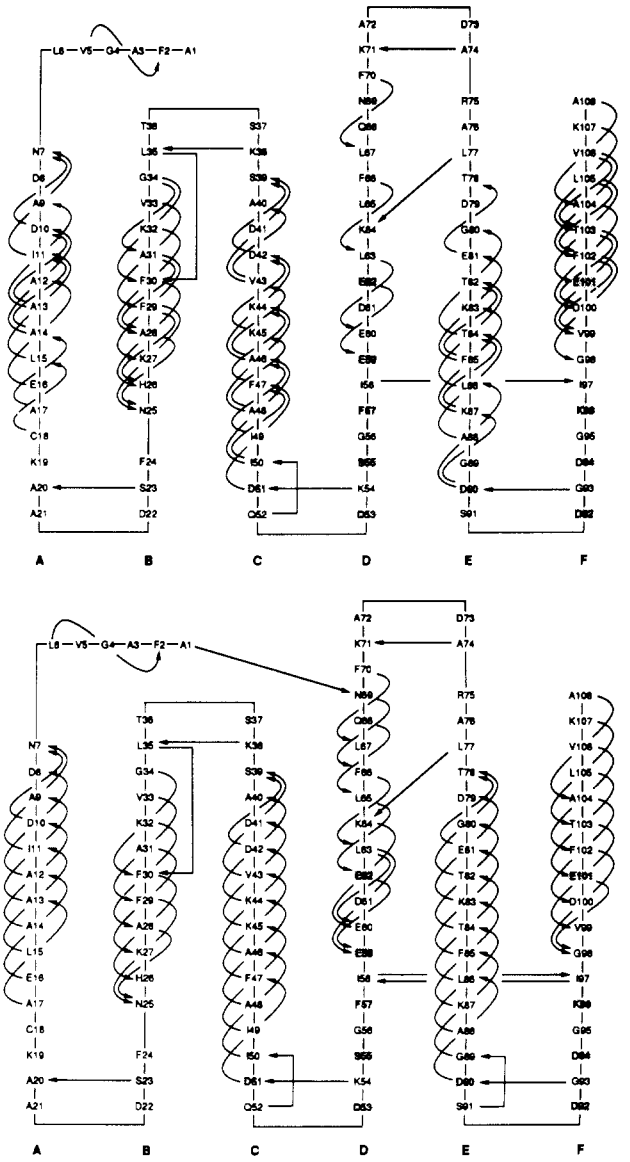

FIGURE 3: Main-chain hydrogen bonds and topology in parvalbumin. The main-chain hydrogen bonds (top) in the 1.9-Å model (Moews & Kretsinger, 1975; F6A coordinates) and (bottom) in the 1.5-Å model of parvalbumin are compared. The criteria for a hydrogen bond are from a review by Baker and Hubbard (1984), namely, the angles C–O···H, O···H–N, and H–N–C must be greater than 90°, and the distance N···O must not exceed 3.3 Å. Residues ligating the calcium ions are shaded.

Table III: Hydrogen Bonds to Side-Chain Atoms[a]

	1.9-Å model		1.5-Å model	
AA[a]	atom 1/ donor[b]	atom 2/ acceptor[c]	atom 1/ donor[b]	atom 2/ acceptor[c]
Asn-7				10-OD2
Asp-8	32-NZ			9-N
Asp-10				7-ND2
Asp-22		78-OG1		
Ser-23			20-O	
Asn-25			27-N, 28-N	
Lys-32	10-OD1, 32-O			
Ser-39		41-N	42-OD2	42-N
Asp-42	45-NZ		45-NZ	39-OG
Lys-45	42-OD1		42-OD1	
Asp-51	54-N	56-N	54-N, 55-N	56-N
Asp-53			55-N	
Lys-54	48-O, 51-O		48-O, 51-O	
Ser-55	57-O, 59-OE2	57-N	57-O, 59-OE2	57-N
Glu-59		55-OG		55-OG
Glu-62		59-N	53-N	59-N
Lys-64	77-O			
Arg-75	76-O	18-O, 81-OE1	76-O, 81-OE2	18-O, 81-OE1
Thr-78	22-OD2		22-OD2	81-N
Glu-81	22-N, 23-N, 75-NH2		78-N	22-N, 24-N, 75-NH1, 78-N
Thr-82	78-O		78-O	
Thr-84	80-O		80-O	
Asp-90	94-N, 95-N	93-N, 94-N	95-N	93-N
Asp-92			94-N	
Asp-94	96-N		96-N	
Glu-101			98-N	91-N, 92-N
Thr-103	99-O		99-O	
Lys-107	36-O, 38-O		38-O	

[a] The atoms involved in hydrogen bonds are identified by the code used in the Brookhaven Data Bank of Macromolecular Structures. For the *n*th residue, *n*–O and *n*–N are the main-chain carbonyl and nitrogen atoms, respectively. The electronegative side-chain atoms are *n*–OD1 and *n*–OD2 for aspartate, *n*–OE1 and *n*–OE2 for glutamate, *n*–NE1, *n*–NH1, and *n*–NH2 for arginine, *n*–OD1 and *n*–ND2 for asparagine, *n*–OE1 and *n*–NE2 for glutamine, *n*–NZ for lysine, *n*–OG for serine, and *n*–OG for threonine. [b] The atoms listed in this column are hydrogen bonded to the *first* electronegative atom (Asp, OD1; Glu, OE1; Arg, NH1; Asn, OD1; Gln, OE1) or the only electronegative atom functioning as a hydrogen bond *donor* (Lys, NZ; Ser, OG; Thr, OG) in the side chain of the residue in the left-hand column. [c] The atoms listed in this column are hydrogen bonded to the *second* electronegative atom (Asp, OD2; Glu, OE2; Arg, NH2; Asn, ND2; Gln, NE2) or the only electronegative atom functioning as a hydrogen bond *acceptor* (Ser, OG; Thr, OG) in the side chain of the residue in the left-hand column.

and 8 peptide nitrogens by our criteria and 48 and 13 by those of Moews and Kretsinger (1975).

The 1.9- and 1.5-Å models differ significantly in their hydrogen-bonding patterns. The helices in the latter are clearly more regular. They contain only seven bifurcated hydrogen bonds, which are restricted to the amino termini. In the 1.9-Å model, there are 19 bifurcated hydrogen bonds distributed throughout the helices. Also, in the 1.5-Å model the hydrogen bonding is continuous in five of six helices, whereas this is true for only two helices in the 1.9-Å model. The hydrogen bonding in the D helix is discontinuous in both models, but it is still more regular in the 1.5-Å structure, in which it contains seven 3_{10} bonds and two α-helical ones as opposed to just four 3_{10} bonds in the 1.9-Å model. Also, the bend at Leu-65 in helix D is less extreme in the 1.5-Å model ($\phi = -96°$, $\psi = 14°$) than in the 1.9-Å model ($\phi = -148°$, $\psi = 78°$).

The other hydrogen bonds in Figure 3 are generally similar. However, the five amino-terminal residues have a 3_{10} bond and a free amino terminus in the 1.9-Å structure but an α-helical bond and an amino terminus bonded to Asn-69 in the 1.5-Å model. Also, the I97→I58 and S91→G89 bonds are absent in the 1.9-Å model. Moews and Kretsinger listed the former but flagged it as unlikely on the basis of their criteria. They also did not accept three extra-helical bonds that QUANTA reports in their structure, namely S23→A20, Q52→I50, and S91→G89.

A total of 15 peptide nitrogen atoms were identified by Moews and Kretsinger (1975) as not making a hydrogen bond either to another residue or to solvent. Eleven of these amide groups (residues 10, 27, 34, 45, 52, 53, 68, 69, 81, 89, and 97) are hydrogen bonded in the 1.5-Å model (Figure 4 and Table III), although five of them (10, 34, 45, 52, and 81) are actually hydrogen bonded in the 1.9-Å structure according to the criteria of Baker and Hubbard (1984).

The crystal packing of parvalbumin is such that each molecule contacts eight neighbors. The only two main-chain intermolecular contacts are made by the amide nitrogens of Ala-72→Asp-92 and Asp-73→Gly-93. There are four side-chain intermolecular contacts involving Asn-7 ND2→Glu-60

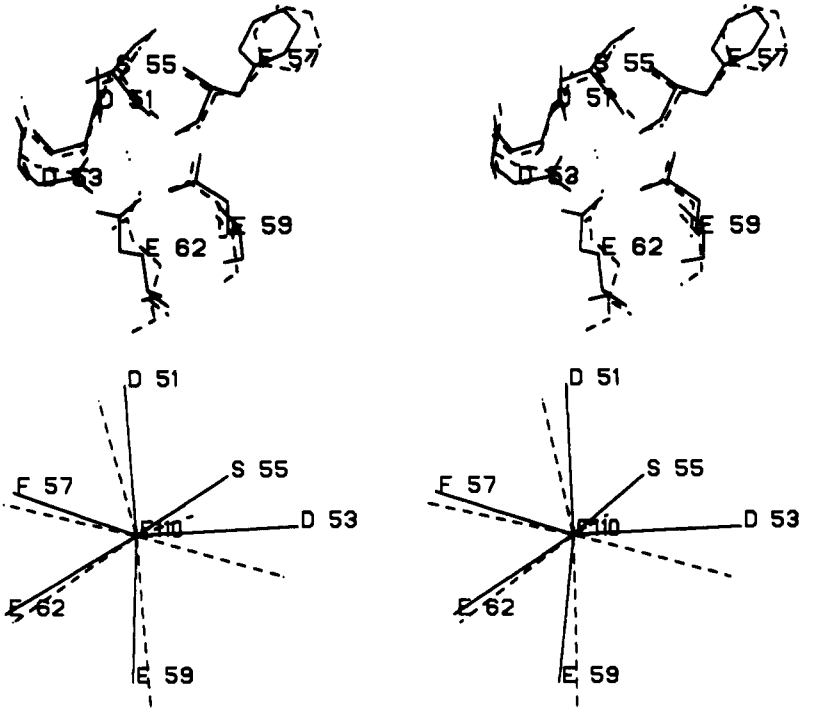

FIGURE 4: Comparison of the CD metal-binding site. (Top) The six residues that form the CD site in the 1.5-Å (solid lines) and 1.9-Å (dashed lines) models are shown in stereo. The least-squares overlap was calculated form the coordinates of all the atoms shown. In the 1.5-Å model Glu-62 ligates the calcium ion with both carboxylate oxygens; in the 1.9-Å model only one is used. The calcium atoms in the two models are indicated by the pair of dots in the center. (Bottom) The metal–oxygen distances for the CD site in the 1.5- (solid lines) and 1.9-Å (dashed lines) models are shown in stereo. The least-squares overlap was calculated from the coordinates of the metal and its oxygen ligands. The structures were then translated to superimpose the metal positions. For Glu-62, the carboxylate atom that was in the most similar position in the two models was used.

Table IV: Comparison of the Calcium–Oxygen Distances of the CD and EF Metal-Binding Site

	CD site			EF site		
site[a]	ligand	1.9 Å[a]	1.5 Å	ligand	1.9 Å[a]	1.5 Å
X	Asp-51 OD1	2.13	2.21	Asp-90 OD2	2.87	2.24
Y_1	Asp-53 OD1	2.35	2.34	Asp-92 OD1	2.48	2.37
Y_2				Asp-92 OD2	2.06	(3.73)
Z	Ser-55 OG	2.42	2.61	Asp-94 OD1	2.63	2.49
$-Y$	Phe-57 O	2.30	2.37	Lys-96 O	2.19	2.42
$-X$	Glu-59 OE1	2.60	2.34	Wat-128 O	2.39	2.35
$-Z_1$	Glu-62 OE1	2.31	2.61	Glu-101 OE1	2.37	2.38
$-Z_2$	Glu-62 OE2	(3.27)	2.40	Glu-101 OE2	2.44	2.69
	av	2.35	2.41		2.43	2.42

[a] From Moews and Kretsinger (1975). Numbers in parentheses are nonbonding distances.

OE1, Asp-8 OD1→Ser-91 OG, Asp-22 O→Asn-25 ND2, and Phe-24 O→Asn-25 ND2. There are also several intermolecular contacts involving water bridges between the molecules. These include the peptide nitrogen of Val-99 and the carbonyl oxygen of Gly-56, the peptide nitrogen of Glu-60 and the carbonyl of Asp-61, and the peptide nitrogen of Gly-95 and the side-chain oxygen of Glu-60.

The hydrogen bonds that involve side-chain atoms as donors, acceptors, or both are compared for both parvalbumin structures in Table IV. In both structures the side chains of the Asx, Glu, Ser, and Thr residues frequently "loop back" to nearby backbone atoms. This pattern, called the "Asx" bond, has been seen in other proteins (Rees et al., 1983; Baker & Hubbard, 1984). Herzberg and James (1985) have proposed that the calcium-binding loops (EF hands) of the type found in parvalbumin contain four Asx hydrogen bonds as part of their consensus structure. In the amino acid sequence of carp parvalbumin 4.25 there are three possible Asx bonds at the CD site (Asp-51, Asp-53, Ser-55) and three at the EF site (Asp-90, Asp-92, Asp-94). In the 1.5-Å model, we actually observe only two Asx bonds at each site (Asp-53, Ser-55; Asp-92, Asp-94). The 1.9-Å model contains only one Asx bond at each site (Ser-55; Asp-94). In the same vein, three of the six glutamate side chains and three of the five threonine side chains in parvalbumin form looped hydrogen bonds—the former to the peptide nitrogen of the n-3 residue, and the latter to the carbonyl oxygen of the n-4 residue.

Calcium Binding Sites. The CD calcium in the 1.5-Å model is coordinated by seven oxygen atoms in a distorted octahedral arrangement. There are six oxygen ligands in the 1.9-Å structure. Figure 4 (top) shows the superposition of the CD metal-binding site from the 1.5- and 1.9-Å structure. The rms deviation between the residue positions is 0.58 Å. The major difference between the two structures is that both carboxylate oxygens of Glu-62 are involved in forming ligands with the metal in the 1.5-Å model, as compared to only one metal–oxygen ligand in the 1.9-Å structure. A seven-coordinate calcium at the CD site has also been observed in the independent refinement of parvalbumin with a lanthanide ion in the EF site (V. Kumar, L. Lee, and B. Edwards, unpublished results). Figure 4 (bottom) shows just the oxygen atoms of the CD metal-binding site in the 1.9-Å model overlapped onto those of the 1.5-Å model with a rms deviation of 0.37 Å. The liganding oxygens of Asp-53 and Ser-55 showed the largest differences in relative position between the two models. The range for the O–Ca^{2+}–O angles was 149–167° for the axial angles (180° in a perfect octahedron) and 75–134° for the nonaxial angles (90° in a perfect octahedron). The rms deviation from the values for a perfect octahedron were 26° and 17°, respectively. The corresponding ranges for the axial and nonaxial angles in the 1.9-Å structure were 113–172° and 75–134°, respectively, with respective rms deviations of 39° and 15° from octahedral values.

The EF calcium is also coordinated by oxygen atoms in a distorted octahedral geometry. Figure 5 (top) shows the su-

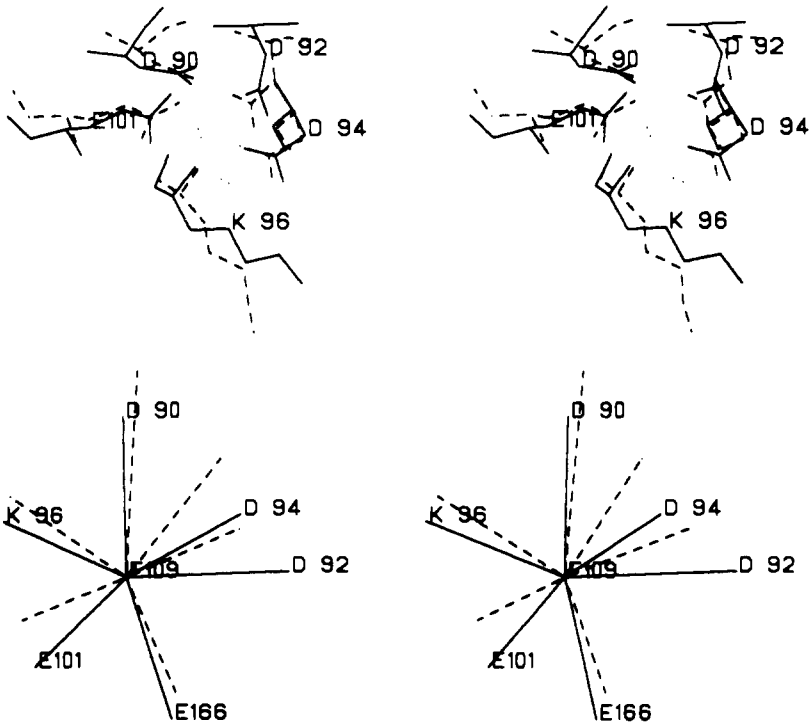

FIGURE 5: Comparison of the EF metal-binding site. (Top) The five residues that form the EF site in the 1.5-Å (solid lines) and 1.9-Å (dashed lines) models are shown in stereo. The least-squares overlap was calculated from the coordinates of all the atoms shown. In the 1.5-Å model Asp-92 ligates the calcium ion with only one carboxylate oxygen; in the 1.9-Å model both are used. Both models have one water molecule ligating the calcium ion. The calcium atom and the water molecule in the two models are represented by the pair of dots in the center and in the lower half of the figure respectively. (Bottom) The metal–oxygen distances for the EF site in the 1.5- (solid lines) and 1.9-Å (dashed lines) models are shown in stereo. The least-squares overlap was calculated from the coordinates of the metal and its oxygen ligands. The structures were then translated to superimpose the metal positions. For Asp-92 and Glu-101, the carboxylate atom that was in the most similar position in the two models was used.

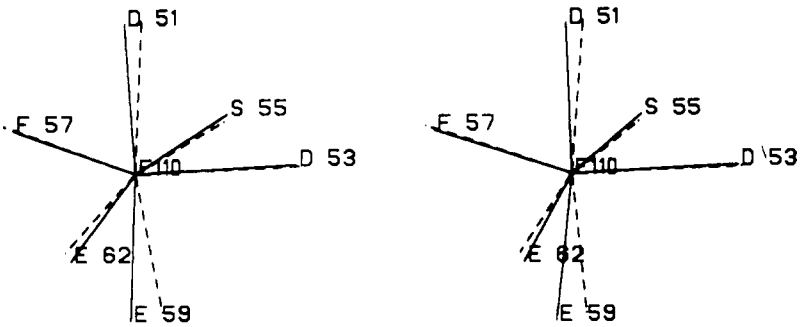

FIGURE 6: Comparison of the CD and EF metal-binding sites. The metal–oxygen distances for the CD (solid lines) and EF (dashed lines) sites in the 1.5-Å model are shown in stereo. The least-squares overlap was calculated from the coordinates of the metal and its oxygen ligands. The structures were then translated to superimpose the metal positions.

perposition of the EF metal-binding site between the two models. The rms deviation was 0.67 Å. As evident from the larger rms deviation in atom position, the EF sites in the two models are less similar in the relative position of their calcium ligands than are the CD sites. Again, the major difference between the two models is the number of oxygen ligands to the calcium ion—in this case a reduction from eight to seven. Only one carboxylate oxygen of Asp-92 binds to the calcium ion in the 1.5-Å model, as compared to two oxygen atoms in the 1.9-Å structure. Figure 5 (bottom) shows just the oxygen atoms of the EF site from the two models overlapped with a rms deviation of 0.47. The range of axial angles was 148–161° and 144–156° in the 1.5- and 1.9-Å models, respectively; the range of nonaxial angles was 74–125° and 58–128°, respectively. The EF site is more octahedral in the 1.5-Å model in that the rms deviations of the angles from ideal values, which were 26° for the axial angles and 16° for the nonaxial ones, are consistently smaller than the respective values of 29° and 23° in the 1.9-Å model.

The change in coordination of the calcium ions from six oxygens in the CD site and eight oxygens in EF site of the 1.9-Å structure to seven oxygens for both sites in the 1.5-Å model is squarely within the range observed for calcium complexes with small ligands and with proteins. In a review of calcium coordination by small ligands, Kretsinger (1976) found that of 17 structures, 12 had 8 oxygens around the calcium ion, 4 had 7 oxygens, and 1 had 6 oxygens. For protein structures, the number of ligands ranges from five to seven (Kretsinger, 1987), but seven ligands predominate in the refined crystal structures of proteins homologous to parvalbumin (Szebenyi & Moffat, 1987; Herzberg et al., 1987; Declercq et al., 1988). Moreover, the changes in calcium coordination observed in the 1.5-Å structure of parvalbumin agree nicely with the pattern seen in sites III and IV of troponin C (Herzberg et al., 1987), site III/IV of vitamin D dependent calcium-binding protein (Szebenyi & Moffat, 1987), and the CD and EF sites of pike parvalbumin 4.10 (Declercq et al., 1988), namely, single side-chain oxygens at

the *X*, *Y*, *Z*, and *−X* positions, a main-chain carbonyl oxygen at the *−Y* position, and two carboxyl oxygens at the *−Z* position. The increased similarity between the CD and EF sites in the 1.5-Å model is responsible for the low rms deviation of 0.22 Å that was calculated when their oxygen ligands were overlapped in Figure 6.

Table IV compares the bond distances for the CD and EF metal-binding sites for the two models. The oxygen-calcium bond distances in the 1.5-Å model range from 2.21 to 2.69 Å with an average for the 14 distances of 2.41 Å. Kretsinger (1976) calculated an average value of 2.40 Å for calcium complexes with seven oxygen atoms.

Thermal Factors. The average *B* value for the main-chain atoms in the 1.5-Å model is 18 ± 7 Å^2 as opposed to 17 ± 14 Å^2 in the 1.9-Å model [F6H coordinates in Moews and Kretsinger (1975); file 2CPV in the Protein Data Bank]. In the 1.5-Å model, the average temperature factor for the main-chain atoms of the individual residues was greater than one standard deviation above the overall average at the amino terminus (residues 1–9), the external loop between the B and C helix (residues 38–41), and the carboxy terminus (residue 108). The average *B* value for the five amino-terminal residues is 40 Å^2 in the 1.5-Å model compared to 62 Å^2 in the 1.9-Å model. Consequently, the amino terminus in our electron density map was better defined. The increased *B* values for residues 38–41 occur near where there is a significant rms difference in atomic positions between the two models. Despite the local mobility in this region, the electron density was straightforward to interpret.

We compared the relative mobility of the main-chain atoms in the 1.5- and 1.9-Å structures by averaging the temperature factors by residue and then expressing them in terms of standard deviations from the overall average temperature factor of each model. These *Z* temperature factors showed approximately the same relative variation along the sequence in both models. They differed by greater than 2 standard deviations only at residues Ala-3, Leu-35, Glu-60, and Lys-87. In all cases, the residues were relatively less mobile in the 1.5-Å model.

Water Molecules. Our interpretation of the water structure after refinement yields 74 ordered water molecules. Thirty-seven water sites have full occupancy, and the rest are partially occupied, the lowest occupancy in the final model being 0.6 for one water than is located on a twofold rotation axis. The high number of fully occupied sites indicates that the water molecules we have placed in the refined structure are highly ordered. Twelve water molecules are found within hydrogen-bonding distance of the backbone amides, and an additional 22 water molecules are within hydrogen-bonding distance of the main-chain carbonyl oxygens. Of the remaining 40 water molecules 18 form at least one hydrogen bond to side-chain nitrogens or oxygens, 11 are involved in forming water–water contacts, 1 is involved in the binding of calcium in the EF metal-binding site, and 10 molecules do not form hydrogen bonds. The 10 water molecules that do not have hydrogen-bonding partners have been included in the analysis because they are ordered and have high occupanices. Comparison of the ordered solvent structures in the two models shows that 9 of 25 ordered water molecules in the 1.9-Å model (F6H coordinates) are located at very similar positions and have same hydrogen-bond partners.

Added in Proof

After the manuscript was submitted for publication, we learned that other researchers have also found calcium to be seven coordinate in the CD and EF sites of carp 4.25 parvalbumin (A. Swain, R. H. Kretsinger, and S. Amma, personal communication).

Acknowledgments

We are indebted to Colin Broughton, Paul Bethge, George Reeke, and Wayne Hendrickson for computer programs used in this study.

Registry No. Ca, 7440-70-2; O_2, 7782-44-7.

References

Baker, E. N., & Hubbard, R. E. (1984) *Prog. Biophys. Mol. Biol. 44*, 97–179.

Berchtold, M. W., Epstein, P., Beaudet, A. L., Payne, M. E., Heizmann, C. W., & Means, A. R. (1987) *J. Biol. Chem. 262*, 8696–8701.

Bernstein, F. C., Koetzle, T. F., Williams, G. J. B., Meyer, E. F., Jr., Brice, M. D., Rodgers, J. R., Kennard, O., Shinanouchi, T., & Tsumi, M. (1977) *J. Mol. Biol. 122*, 535.

Brewer, J. M., Wunderlich, J. K., Kim, D.-H., Carr, M. Y., Beach, G. G., & Ragland, W. L. (1989) *Biochem. Biophys. Res. Commun. 160*, 1155–1161.

Celio, M. R. (1986) *Science 231*, 995.

Coffee, C. J., & Bradshaw, R. A. (1973) *J. Biol. Chem. 248*, 3305.

Coffee, C. J., Bradshaw, R. A., & Kretsinger, R. H. (1974) *Adv. Exp. Med. Biol. 48*, 211–233.

Creighton, T. E. (1984) *Proteins, Structures and Molecular Properties*, Freeman, New York.

Declercq, J.-P., Tinant, B., Parello, J., Etienne, G., & Huber, R. (1988) *J. Mol. Biol. 202*, 349–353.

Deuticke, H. J. (1934) *Z. Phys. Chem. 224*, 216–218.

Diamond, R. (1971) *Acta Crystallogr. A27*, 436.

Frankenne, F., Joassin, L., & Geraday, C. (1973) *FEBS Lett. 35*, 145–147.

Hamoir, G. (1951) *Biochem. Soc. Symp. 6*, 8–27.

Heizmann, C. W., & Strehler, E. E. (1979) *J. Biol. Chem. 254*, 4296.

Hendrickson, W. A., & Konnert, J. H. (1980) in *Computing in Crystallography* (Diamond, R., Ramaseshan, S., & Venkatesan, K., Eds.) Indian Academy of Sciences, International Union of Crystallography, Bangalore, India.

Herzberg, O., & James, M. N. G. (1985) *Biochemistry 24*, 5298–5302.

Herzberg, O., Moult, J., & James, M. N. G. (1987) *Methods Enzymol. 139*, 610–633.

Kahn, R., Fourme, R., Bosshard, R., Chiadmi, M., Risler, J. L., Dideberg, O., & Wery, J. P. (1985) *FEBS Lett. 179*, 133–137.

Kannan, K. K., Liljas, A., Warra, J., Bergsten, P. C., Lovgren, S., Bengtsson, U., Carlbom, U., Fridborg, K., Jarup, L., Petef, M., & Stranberg, N. (1971) *Cold Spring Harbor Symp. Quant. Biol. 36*, 221–231.

Konusu, S., Hamoir, G., & Pechêre, J. F. (1965) *Biochem. J. 96*, 98–112.

Kretsinger, R. H. (1976) *Coord. Chem. Rev. 18*, 29–124.

Kretsinger, R. H. (1980) *CRC Crit. Rev. Biochem. 8*, 119–174.

Kretsinger, R. H. (1987) *Cold Spring Harbor Symp. Quant. Biol. 52*, 499–510.

Kretsinger, R. H., & Nockolds, C. E. (1973) *J. Biol. Chem. 248*, 3313–3326.

Lee, L., & Sykes, B. D. (1983) *Biochemistry 22*, 4366–4373.

McPherson, A. (1982) *Preparation and Analysis of Protein Crystals*, Wiley, New York.

Moews, P. C., & Kretsinger, R. H. (1975) *J. Mol. Biol. 91*, 201–235.

Nockolds, C. E., Kretsinger, R. H., Coffee, C. J., & Bradshaw, R. A. (1972) *Proc. Natl. Acad. Sci. U.S.A. 69*, 581-584.
North, A. C. T. (1965) *Acta Crystallogr. 18*, 212.
Pechère, J. F., Demaille, J., & Capony, J. P. (1971) *Biochim. Biophys. Acta 236*, 391-408.
Pechère, J. F., Capony, J. P., & Demaille, J. (1973) *Syst. Zool. 22*, 533-548.
Rao, K. S. P., & Geraday, C. (1973) *Comp. Biochem. Physiol. 44*, 931.
Reeke, G. N. (1984) *J. Appl. Crystallogr. 17*, 125.
Rees, D. C., Lewis, M., & Lipscomb, W. N. (1983) *J. Mol. Biol. 168*, 367-387.
Rossmann, M. G., & Argos, P. (1975) *J. Biol. Chem. 250*, 7525.
Sielecki, A. R., James, M. N. G., & Broughton, C. G. (1982) in *Crystallographic Computing* (Sayre, D., Ed.) p 409, Oxford University Press, London.
Stuhfauth, I., Reininghaus, J., Jockusch, H., & Heizman, C. W. (1984) *Dev. Biol. 128*, 4814-4818.
Szebenyi, D. M. E., & Moffat, K. (1987) *Methods Enzymol. 139*, 585-611.
Wyckoff, H. W., Doscher, M. S., Tsernoglou, D., Ingami, T., Johnson, L. N., Hardman, K. D., Allewell, N. M., Kelley, D. M., & Richards, F. M. (1967) *J. Mol. Biol. 127*, 563.

Specificity of *S*-Adenosylmethionine Synthetase for ATP Analogues Mono- and Disubstituted in Bridging Positions of the Polyphosphate Chain†

Qi-Feng Ma,‡ George L. Kenyon,*,‡ and George D. Markham*,§

Department of Pharmaceutical Chemistry, University of California, San Francisco, California 94143, and Institute for Cancer Research, Fox Chase Cancer Center, 7701 Burholme Avenue, Philadelphia, Pennsylvania 19111

Received August 15, 1989; Revised Manuscript Received October 2, 1989

ABSTRACT: The entire family of ATP analogues that are either mono- or disubstituted with imido and methylene bridges in the polyphosphate chain of ATP have been investigated as substrates and inhibitors of *S*-adenosylmethionine synthetase (ATP:L-methionine *S*-adenosyltransferase). The disubstituted analogues adenosine 5′-(α,β:β,γ-diimidotriphosphate) (AMPNPNP) and adenosine 5′-(α,β:α,β'-diimidotriphosphate) [AMP(NP)$_2$] have been synthesized for the first time, and a new route to adenosine 5′-(α,β:β,γ-dimethylenetriphosphate) (AMPCPCP) has been developed. *S*-Adenosylmethionine synthetase catalyzes a two-step reaction: the intact polyphosphate chain is displaced from ATP, yielding AdoMet and tripolyphosphate, followed normally, but not obligatorily, by the hydrolysis of the tripolyphosphate to pyrophosphate and orthophosphate. Uniformly, the imido mono- or disubstituted derivatives are both better substrates and better inhibitors than their methylene counterparts. AMPNPNP reacts rapidly to give a single equivalent of product per active site, but subsequent turnovers are at least 1000-fold slower, enabling it to be used to quantify enzyme active site concentrations. In contrast, AMPCPCP is not detectably a substrate ($<10^{-5}$% of ATP). AMP(NP)$_2$, a branched isomer of linear AMPNPNP, was not a substrate but was a linear competitive inhibitor, >100 fold more potent than ADP, indicating a reasonable degree of bulk tolerance at the α-phosphoryl group binding site. Adenosine 5′-(α,β-imidotriphosphate) (AMPNPP) is a surprisingly potent inhibitor as well as substrate, with an inhibition constant that is ~60-fold less than the K_m for ATP, and is an ~1000-fold better inhibitor than adenosine 5′-(α,β-methylenetriphosphate) (AMPCPP). These findings reinforce the notion that imido analogues of ATP are more suitable analogues of ATP than their corresponding methylene compounds.

The only known biosynthetic route to *S*-adenosylmethionine arises from a reaction catalyzed by *S*-adenosylmethionine synthetase. *S*-Adenosylmethionine (AdoMet) synthetase (ATP:L-methionine *S*-adensoyltransferase) catalyzes a two-step reaction in which ATP and methionine first combine to form AdoMet and tripolyphosphate; the tripolyphosphate is then hydrolyzed to PP_i and P_i (which originates as the γ-phosphoryl group of ATP) before product release (Mudd, 1973; Tabor & Tabor, 1984). In the presence of the ATP analogue AMPPNP[1] multiple turnovers of AdoMet formation can occur without polyphosphate bond cleavage (Markham et al., 1980); therefore, AdoMet synthetase is a rare enzyme for which the influence of substitution in both the α,β- and the β,γ-bridging positions of the polyphosphate chain of ATP on enzyme affinity and activity can be assessed. Furthermore, there is the possibility that an ATP analogue containing nonhydrolyzable bonds in both the α,β- and β,γ-bridges would

† This work was supported by U.S. Public Health Service Grants GM-39552 and AR-17323 (to G.L.K.), GM-31186 (to G.D.M.), and CA-06927 and RR-05539 (to the Fox Chase Cancer Center) and also an appropriation from the Commonwealth of Pennsylvania.

‡ University of California, San Francisco.
§ Fox Chase Cancer Center.

[1] Abbreviations: AMPNPNP, adenosine 5′-(α,β:β,γ-diimidotriphosphate); AMP(NP)$_2$, adenosine 5′-(α,β:α,β'-diimidotriphosphate); PNPNP, diimidotriphosphate; AMPNP, adenosine 5′-(α,β-imidodiphosphate); AMPNPP, adenosine 5′-(α,β-imidotriphosphate); AMPPNP, adenosine 5′-(β,γ-imidotriphosphate); PCPCP, bis[(dihydroxyphosphinyl)methyl]phosphinate; AMPCPCP, adenosine 5′-(α,β:β,γ-dimethylenetriphosphate); AMPCPP, adenosine 5′-(α,β-methylenetriphosphate); AMPPCP, adenosine 5′-(β,γ-methylenetriphosphate); AMP(CP)$_2$, adenosine 5′-(α,β:α,β'-dimethylenetriphosphate); AMP(OP)$_2$, adenosine 5′-(α,β:α,β'-triphosphate); PEI, poly(ethylenimine); LSIMS, liquid secondary ion mass spectrometry; SP, sulfopropyl; TEA, triethylammonium; QAE, quaternary aminoethyl; DEAE, diethylaminoethyl.

0006-2960/90/0429-1412$02.50/0